Journal of Alloys and Compounds, 195 (1993) 711–714
JALCOM 7564

On-chip diagnostic of high-T_c superconductors at mm-wave frequencies

J. Edstam[a], P-Å. Nilsson[a], E. A. Stepantsov[b], and H. K. Olsson[a]

[a] Department of Physics, Chalmers University of Technology, S-412 96 Göteborg, Sweden

[b] Institute of Crystallography, Russian Academy of Sciences, 59 Leninskii pr., 117333 Moscow, Russia.

Abstract

We have fabricated and operated a basic integrated high-T_c device consisting of an active Josephson junction oscillator and a passive microstrip resonator. By using a junction self-detection technique, material related parameters such as surface resistance and London penetration depth could be directly extracted from the IV-curve. Due to the intrinsic large bandwidth of the Josephson junction oscillator (~$2eI_oR/h$ where I_o and R are the junction critical current and resistance, respectively) we have been able to make measurements of YBCO in the frequency range 80-220 GHz. We anticipate that even higher frequencies can be used to probe these materials by taking full use of high-T_c Josephson junctions.

1. Introduction

The high frequency response of superconductors is of fundamental interest for the understanding of superconductivity and is also important for a range of applications using superconductors. Low-T_c superconducting materials have added extra performance to microwave detectors, filters, digital circuits, etc.[1,2] compared to their semiconducting/metallic counterparts. Advantages have been taken of the low loss, low dispersion, and high characteristic frequency of superconductors and Josephson junctions. A problem has been to make measurements in the interesting gap between the microwave[3] and the FIR[4] (Far Infra Red) frequency ranges due to lack of standard instrumentation.

We report the use of integrated on-chip high-T_c Josephson junctions and microstrips[5] to measure the surface resistance, London penetration depth, phase velocity, dispersion etc. in the frequency range 80-220 GHz. Such circuits have previously been studied using low T_c superconductors at mm-wave frequencies[6,7,8] but now for the first time using high-T_c superconductors. Time domain analysis have also been used to study fast response[9].

2. Theory

The Josephson junction is a voltage controlled oscillator with a frequency proportional to the applied voltage: $f=2eV/h=484$ GHz/mV, and with an intrinsically high characteristic frequency: $f_c=2eI_oR/h$. The biased junction, positioned in the middle between two open ended microstrips, will send out a traveling wave with propagation constant, $\beta=2\pi/\lambda$, and attenuation constant, α, onto the microstrip. The impedance seen by the junction is then given by $Z=2Z_o \coth[(\alpha+j\beta)l/2]$, where $Z_o=\sqrt{L/C}$ is the microstrip impedance and l is its total length, see Figure 1[10]. The microstrip thus adds a parallel resistance whenever the Josephson frequency equals the microstrip resonance frequencies,

$$f_n=n\, v_p/2l \qquad n=1,3,5,... \qquad (1)$$

where $v_p=1/\sqrt{LC}$ is the phase velocity[5]. The inductance per unit length, L, of a superconductor is given by $L=\mu_o[d+2\lambda_L(T)\coth(t/\lambda_L(T))]/w$, where d is the dielectric thickness, $\lambda_L(T)$ the London penetration depth, and t is the film thickness. The capacitance per unit length $C=w\varepsilon_o\varepsilon_r/d$. Since the resonance lowers the load resistance, less power will be drawn from the junction which is observed as a dip in current at voltages $hf_n/2e$.

The magnitude of the dip in dimensionless units is given by $\Delta I_S/I_{SO} = 1/(1+R_Sl/Rw)$, if harmonic components of the Josephson frequency are ignored. I_{SO} is the supercurrent without Z connected. At frequencies above f_c, harmonic components are small.

The resonance width is proportional to the inverse of the quality factor,

$$Q=\pi Z_o/2(R+R_Sl/w), \qquad (2)$$

where $R_S=Z_o\alpha w$ is the surface resistance and w the microstrip width.

From inspection of the IV-curve it is thus possible to

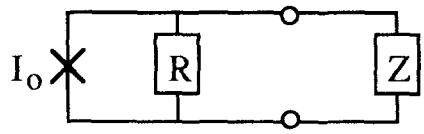

Figure 1. The Josephson junction with critical current I_o and resistance R is connected to two open ended microstrip resonators with a total frequency dependent impedance Z.

0925-8388/93/$06.00

calculate both λ_L and R_S from the position and shape of the dip. Both frequency and temperature can be varied.

3. Experimental

A schematic view of the resonator and Josephson junction is shown in Figure 2, and has been described more in detail earlier[5]. In short, we have used YSZ bicrystal substrates to form artificial grain boundary Josephson junctions in the center of a laser ablated YBCO microstrip (t=0.13 μm, w=10 μm, and l=250 μm). For ease of fabrication we have used an SiO dielectric layer (d=0.4 μm) and either Pb (t=0.3 μm) or Au (t=0.3 μm) as ground plane (w=30 μm) on top of the YBCO.

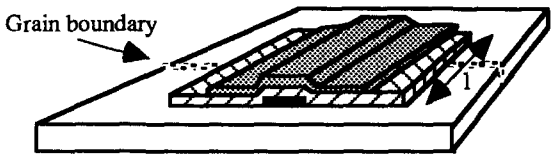

Figure 2. Schematic view of the microstrip resonator with the grain boundary Josephson junction in the center. Black color represents YBCO, hatched SiO, gray Pb or Au, and white the YSZ bicrystal substrate.

4. Results

We will here focus on data taken using Pb as groundplane though no difference in measurement technique or interpretation exist in comparison with the data using Au as groundplane[5].

4.1. IV-curves

Figure 3a shows a set of IV-curves taken at 4.2 K for different applied magnetic flux to a junction ($<\Phi_O=h/2e$). The junction is connected to a 250 μm long microstrip resonator. By tuning the field we could find the optimum critical current in order to more clearly observe the resonance dip in current. A too large I_O made the dip too deep and impossible to fully map out. On the other hand IV's with too small I_O were smeared by thermal noise. A resonance dip is clearly seen in the IV's centered at 198 μV corresponding to 96 GHz. dV/dI-V curves were taken using a lock-in amplifier and are shown in Figure 3b for the same curves as Figure 3a. The resonance produces a positive peak in dV/dI and then a negative peak as the voltage is increased through the resonance. More structure is revealed in the dV/dI's than in the IV's and in this example a second resonance becomes clear at 100 μV or half the voltage of the large resonance. This structure is probably due to a harmonic of the Josephson frequency sensing the resonance at 100 μV.

A more direct method to view the dip was to fit the IV's to an RSJ-curve ($V=R\sqrt{I^2-I_O^2}$) and subtract the two curves. Figure 4 shows such a fit and the difference current ΔI_S for the junction in Figure 3. Though not as rich in detail, we find this method to be the most direct to display the resonant structures.

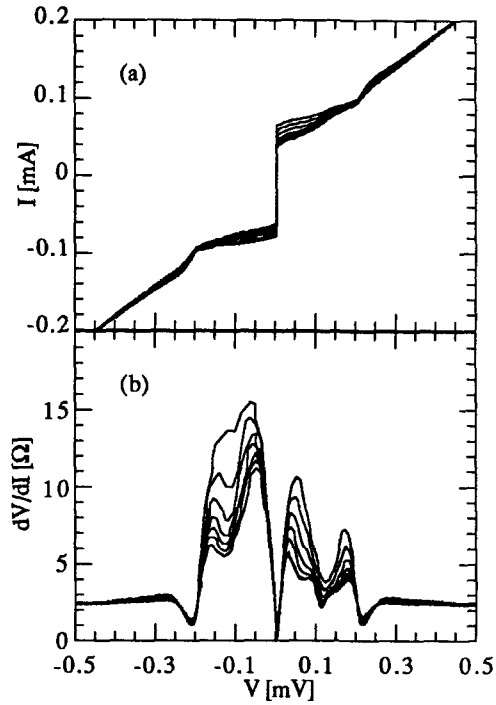

Figure 3. IV- and dV/dI-curves of a YBCO/SiO/Pb resonator for some selected flux biases. The asymmetry is due to trapped flux in the junction vicinity. l= 250 μm, $I_O(\Phi=0)$ = 0.28 mA, and T= 4.2 K.

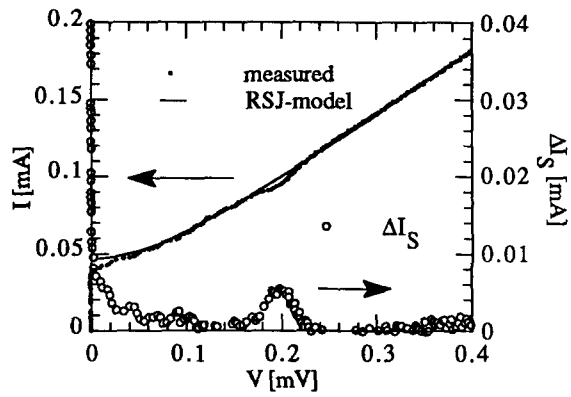

Figure 4. An RSJ-model fit to the measured IV-curve gives the junction IV-curve without external circuitry connected. The difference current, ΔI_S, contains information on the frequency response (f=2eV/h) of the circuitry connected to the junction. T= 4.2 K and l= 250 μm.

4.2 Frequency spectra

We choose to plot the frequency spectra of $\Delta I_S/I_{SO}$, where $I_{SO}=\{\sqrt{I_O^2+(V/R)^2}\}-V/R$ is the supercurrent part of the RSJ-curve, and transferring voltage to frequency using the Josephson relation f=2eV/h. Figure 5 shows

three such spectra for three lengths of the groundplane: l =250, 116, and 0 μm. The YBCO length is in all cases 250 μm. Compared to the full length resonator, the mixed length microstrips displayed additional peaks in their spectra. For l=116 μm, we see an additional weak peak centered at 133 GHz while the microstrip resonance has moved in accordance with the shorter length from 96 GHz to 215 GHz. Fully removing the groundplane (l=0) leaves the weak resonance at 123 GHz which we would like to identify with a parasitic resonance due to the YBCO interacting with its surroundings as a dipole antenna. A uniform YSZ surrounding (ε_r =27) would give a dipole resonance at 115 GHz, close to the observed value.

At higher temperatures, the peaks in the frequency spectra occur at lower frequencies, broaden in width, and reduce in height, see Figure 6. These changes can be directly related to increased values of R_S and λ_L at higher temperatures.

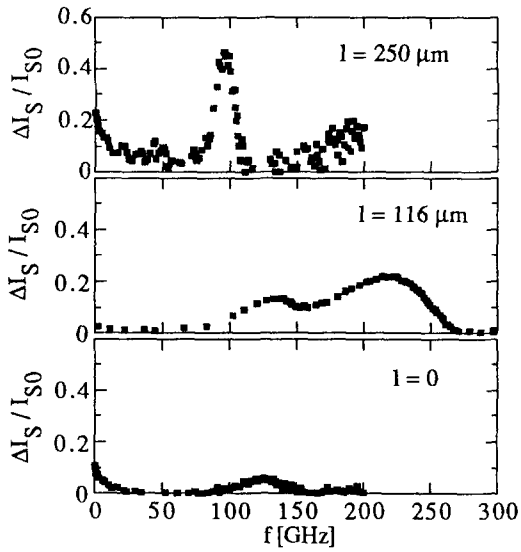

Figure 5. Frequency spectra for different groundplane lengths, l, and fixed YBCO length = 250 μm. Note the change in position of the microstrip resonance between the upper two curves: from 96 to 215 GHz. f_c= 51, 233, and 122 GHz for l= 250, 116, 0 μm, respectively. T=4.2 K.

4.3 Surface resistance

Using the Q-values obtained from the spectra and equation (2), we have calculated the surface resistance of YBCO in the range 100-220 GHz as shown in Figure 7. Though few data points are available at this stage we get approximately $R_S \sim f^{2.0}$. The two fluid model would give an exponent of 2 and is consistent with earlier measurements in the microwave regime[3,9]. For comparison, the thick film surface resistance has also been plotted and is about a factor 4 lower than for our 1300 Å thick film. At 100 GHz we get R_S=10 mΩ in the thick film limit.

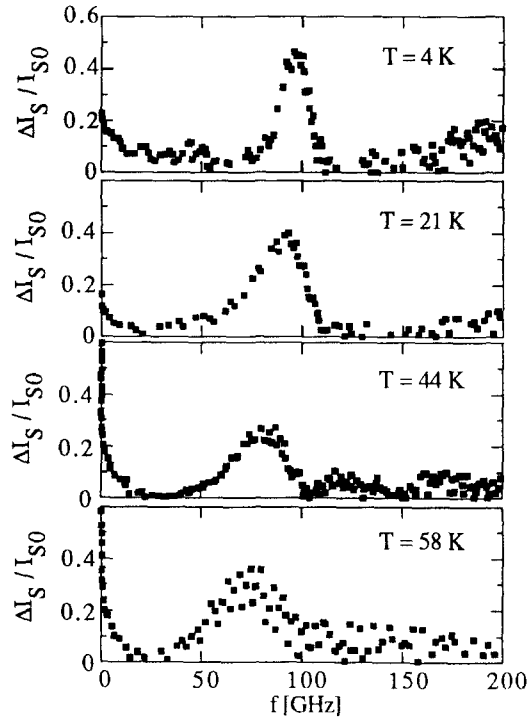

Figure 6. Frequency spectra for four temperatures. The characteristic frequency for these plots were starting from the top of the figure: 51, 82, 54, and 39 GHz, respectively. l= 250 μm.

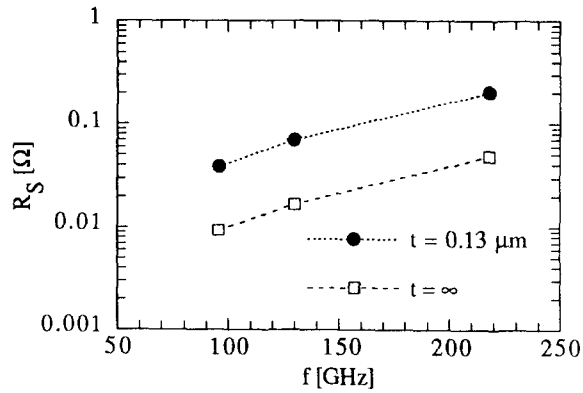

Figure 7. Calculated surface resistance of YBCO at 4.2 K. t = 0.13 μm for the upper and t = ∞ for the lower curve.

4.4 Penetration depth

We have also demonstrated extraction of penetration depth data from the position of the resonance's. Films that are thin compared to the penetration depth will have $L \sim \lambda_L(T)^2/t$ and therefor a strong $f_1(T)$ dependence.

Figure 8 shows calculated values of $\lambda_L(T)$ for three lengths: l=250, 200, and 116 μm. The corresponding change in $f_1(T)$ going from 4.2 to 58 K is about 30% and easily detected. Previously measured values of ε_r =5.5 in this frequency range were used in the calculations[6]. Tabulated values of λ_L(T=4.2 K) are lower (~2000 Å)

than our value of ~5000 Å. We expect that the accidental low $T_C \approx$ 80 K of this film have resulted in an increased penetration depth.

The dispersion over this frequency range (~100-200 GHz) is determined by the frequency dependence of λ_L and practically non-existent or close to the relative accuracy of the data-points, i.e. ~10^{-2}.

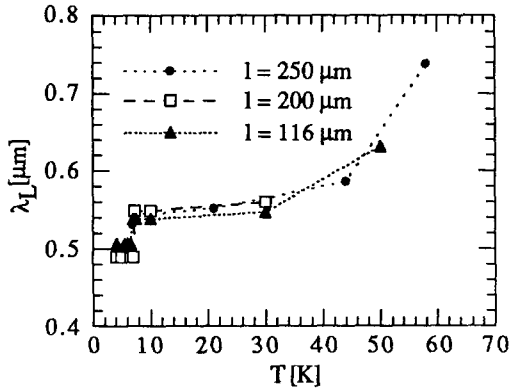

Figure 8. Calculated temperature dependence of the London penetration depth at three lengths of the Pb groundplane. The inductive change of Pb at its T_C= 7.2 K has been ignored.

5. Summary

We have demonstrated a simple on-chip method to evaluate material properties of high-T_C superconductors at mm-wave lengths. The method uses resonance's of open ended YBCO/SiO/(Pb or Au) microstrip lines that are detected in the IV-curve of a YBCO Josephson junction. The surface resistance and London penetration depth were calculated from the measured Q-values and frequency of the resonance's, respectively. With this method we could cover the frequency range 80-220 GHz and measure at temperatures from 4 to 80 K.

Acknowledgments

This work has been supported by "Swedish Research Council for Engineering Sciences", "The Swedish Research Council for Planning and Coordination of Research", and "The Swedish Board for Industrial and Technical Development". The use of the Swedish Nanometer Laboratory is gratefully acknowledged.

References

1 P. L. Richards, and Q. Hu, Proc. IEEE, 77, 1233, (1989).
2 K. K. Likharev, and V. K. Semenov, IEEE Trans. Appl. Superconductivity, 1, 3, (1991).
3 J. S. Martens, G. K. G. Hohenwarter, D. P. McGinnis, J. B. Beyer, and D. S. Ginley, IEEE Trans. Magn., MAG-25, 984, (1989).
4 D. Miller, P. L. Richards, S. Etemad, A. Inam, T. Venkatesan, B. Dutta, X. D. Wu, C. B. Eom, T. H. Geballe, N. Newman, and B. F. Cole, Appl. Phys. Lett., 59, 2326, (1991).
5 J. Edstam, P-Å. Nilsson, E. A. Stepantsov, and H. K. Olsson, Appl. Phys. Lett., to be published.
6 H.K. Olsson, IEEE Trans. Magn., MAG-25, 1115, (1989)
7 H. H. S. Javadi, W. R. McGrath, B. Bumble, H. G. LeDuc, unpublished.
8 B. Bi, K. Wan, W. Zhang, S. Han, and J. E. Lukens, IEEE Trans. on Applied Superconductivity, 1, 145, (1991).
9 M. C. Nuss, K. W. Goossen, P. M. Mankiewich, M. L. O'Malley, J. L. Marshall, and R. E. Howard, IEEE Trans. Magn., MAG-27, 863, (1991).
10 R.C.Collins, Foundations for Microwave Engineering, McGraw-Hill, London, 1966.